Microbial composition, diversity, and activity varies across different types of basal ice

Shawn M. Doyle[a] and Brent C. Christner[b]

[a]Department of Oceanography, Texas A&M University, College Station, TX, USA.
[b]Department of Microbiology and Cell Science, University of Florida, Gainesville, FL, USA.

Running title: **Microbial ecology of different basal ice types**

Abstract word count: 214
Main text word count: 6579

*Corresponding author:
Shawn M. Doyle
Department of Oceanography
Texas A&M University
Eller O&M Bldg, Rm 716D
College Station, TX, 77843-3146
Tel: 979-845-5105
E-mail: shawndoyle@tamu.edu

Competing Interests: The authors declare no competing financial interests.

ABSTRACT

Basal ice often contains entrained subglacial debris and sediment which can serve as a source of nutrients and organic matter and provide habitat for microorganisms adapted to frozen conditions. However, basal ice comes in many different forms and comparatively little is known about how microbial composition, diversity, and activity vary across different types of basal ice. Here, we investigated these parameters in four different types of basal ice from two different glaciers and then used a meta-analysis to compare our findings with microbiome studies of other permanently frozen environments. We found microbiome composition varies substantially between basal ice types, even within the same glacier. Further, the microbiomes of sediment-rich basal ices were distinct from those found in glacial ice and instead were most like those found in permafrost. Consistent with this, microbial diversity was also comparable to that found in permafrost and was much higher relative to glacial ice. Patterns of 16S rRNA read abundance from RNA relative to DNA implicated certain taxa as potentially active in basal ice with ice temperature appearing to be an important predictor for the diversity of taxa inferred to be active. Our results improve our understanding of the microbial ecology of different basal ice types and provide insight into which types are likely habitats for metabolizing microbial communities.

1. INTRODUCTION

Basal ice has a chemistry and physical structure that is directly affected by its proximity to and interaction with material beneath the glacier (Knight, 1997). Basal ice layers are typically entrained with debris from the underlying substrate that ranges in size from fine-grained clays and silts to coarse sands, gravels, and boulders. Basal ice formation can produce layering and stratification patterns that become deformed by the folding and shearing forces associated with glacier flow. These processes of entraining and restructuring of subglacial debris combine to produce various types of basal ice. This ranges from relatively debris-poor types containing <1% (w/v) sediment to debris-rich types composed almost entirely of sediment with only interstitial ice (Knight, 1997). When compared to overlying englacial ice (i.e., derived from snowfall and deposited aerosols), the sediment-rich basal ice contains higher concentrations of microbial substrates such as formate, acetate, ferrous iron, and ammonia (Skidmore *et al.*, 2000; Wadham *et al.*, 2004; Tung *et al.*, 2006; Yde *et al.*, 2010). These compounds are hypothesized to be an important source of electron donors for heterotrophic and lithotrophic microorganisms entrapped in subglacial environments, including the basal ice itself (Montross *et al.*, 2013, 2014).

Before there was much interest in the microbiology of the cryosphere, basal ice microbial communities were assumed to exist in a persistent state of metabolic dormancy while frozen. This view began to change around the turn of the century after mounting evidence from several pioneering studies revealed microorganisms are not only abundant in subglacial environments but actively participate in weathering processes (Sharp *et al.*, 1999; Skidmore *et al.*, 2000; Tranter *et al.*, 2002, 2005; Sheridan *et al.*, 2003; Miteva *et al.*, 2004; Yung *et al.*, 2007). The metabolic activity of basal ice microorganisms is now thought

to play an important role not only in the biogeochemistry of basal ice but also downstream terrestrial, freshwater, and marine environments which receive seasonal discharges of basal meltwater (Wadham *et al.*, 2010; Barker *et al.*, 2018; Hopwood *et al.*, 2019; Vick-Majors *et al.*, 2020). Indeed, basal meltwater is one of the largest sources of labile dissolved organic carbon and iron to coastal oceans adjacent to glaciated watersheds (Hood *et al.*, 2009; Bhatia *et al.*, 2013).

Due to accelerated rates of melt in many regions, basal ice microorganisms may also play an important role in global carbon cycling. The Greenland and Antarctic Ice sheets alone are estimated to contain ~10.2 Pg of organic carbon (Priscu *et al.*, 2008), ~0.5% of the estimated world's total soil organic carbon pool (Batjes, 2014). The subglacial production of biogenic methane and its subsequent release during periods of ice sheet retreat could represent a positive feedback mechanism that accelerates further climate warming (Wadham *et al.*, 2012). Indeed, basal ice sediments from John Evans Glacier (Skidmore *et al.*, 2000) and Robertson Glacier (Boyd *et al.*, 2010) have been found to contain viable methanogens and methanotrophy has been documented in subglacial water from the Greenland (Dieser *et al.*, 2014) and Antarctic ice sheets (Michaud *et al.*, 2017). Microbial activities in the subglacial and basal ice zones of the world's glaciers and ice sheets may thus be an overlooked component of Earth's climate oscillations over geologic timeframes. Despite this potential importance, accessing the basal zone of glaciers is logistically difficult and our understanding of basal ice microorganisms and how their composition and activity varies between different types of basal ice is still limited.

In this study, we used 16S rRNA gene amplicon sequencing to profile the composition and structure of microbial assemblages within several different basal ices and

115 RNA-based approaches to identify potentially active taxa. To explore how these microbial
116 assemblages compare to those in other permanently frozen environments, we performed a
117 meta-analysis that combined our data with that from other studies. Many of these studies
118 sequenced different variable regions of the 16S rRNA gene (e.g. V4, V2, V3V4) that do not
119 fully overlap, hindering the use of traditional OTU-based approaches. To address this, we
120 used the SATé-enabled phylogenetic placement (SEPP) technique to insert exact amplicon
121 sequence variants (ASVs) from these heterogenous variable regions into the same
122 reference phylogeny (Janssen *et al.*, 2018). This enabled a phylogenetically stable
123 comparison of the microbial assemblages inhabiting these different frozen environments.
124 In contrast to the aeolian-source microbes in englacial ice, the microorganisms in basal ice
125 appear to represent "communities" in an ecological sense. We discuss the implications of
126 microbial processes in an important transient environment of the cryosphere.
127

128 **2. METHODS AND MATERIALS**

129 **2.1 Ice sampling**

130 *Taylor Glacier*

131 Taylor Glacier is an outlet glacier of the East Antarctic Ice Sheet that terminates at
132 the western end of Taylor Valley (McMurdo Dry Valleys, Victoria Land, Antarctica). During
133 the austral summers of 2007 and 2009, two subglacial tunnels were excavated into the
134 basal zone of the northern lateral margin of the glacier (Figure S1). The tunnels were
135 initiated on fresh ice aprons and extended ~8 m in from the glacier face. At the end of each
136 tunnel, a vertical shaft (2007 expedition) or large chamber (2009 expedition) was
137 excavated to expose a stratigraphic sequence of multiple basal ice types (Montross et al.

2014). Electric chainsaws equipped with unlubricated carbide tipped chains were used to collect samples of the ice sequence from each basal ice type. Ice samples were wrapped in plastic, packed into insulated containers, and shipped frozen to Louisiana State University where they were subsequently stored at -20 °C.

Matanuska Glacier

Matanuska Glacier is a 43km valley glacier located in south-central Alaska, approximately 140 km northeast of Anchorage. In July 2013, a horizon of debris-rich basal ice exposed near the glacier terminus was sampled using an electric chainsaw (Figure S2). After collection, the ice samples were packaged in polypropylene flat wrap and shipped frozen to Louisiana State University for storage at -20 °C.

2.2 Ice decontamination

Within a temperature-controlled laboratory (-5°C), ~2 kg subsamples were cut from large samples of the basal ice using either a band saw (for the sediment-poor basal ice) or a diamond-bladed masonry saw (sediment-rich basal ice). The surface of the freshly cut samples was then cleaned following previous methods (Christner *et al.*, 2005). Briefly, the outermost surface was physically removed by scraping with an autoclaved microtome blade and the newly exposed ice surface was then washed with chilled (-5°C), 0.22 μm filtered 95% ethanol. Microtome scraping was omitted when processing sediment-rich samples due to the presence of coarse granules and stones embedded in the sediment-layers. Following the ethanol wash, samples were washed extensively with ice-cold, 0.22 μm, twice-autoclaved deionized water until a minimum of ~5 mm of the outer surface had been removed based on the ice weight. Large, sterilized surgical forceps were used to handle all ice samples during decontamination and were exchanged frequently during the

161 procedure to prevent carryover contamination. Sample weights before and after
162 decontamination were used to estimate the amount of material removed from each sample
163 during processing, which was typically between 15% and 25% of the initial mass.
164 The effectiveness of the decontamination procedure was monitored by coating ice
165 samples beforehand with a tracer solution that consisted of three components: (1) ~10^8
166 cells mL^{-1} of *E. coli* JM109 cells transformed with a pETBlue-2 plasmid (Novagen)
167 containing the gene for alcohol dehydrogenase (ADH) from *Drosophila melanogaster*, (2)
168 fluorescein (1000 ppm), and (3) 33% (v/v) glycerol to prevent freezing on the ice at -5°C.
169 The removal of the tracer was monitored after each step of the decontamination procedure
170 (i.e. scraping, ethanol wash, H_2O wash). The fluorescein fluorophore component was
171 monitored by quantifying blue-green fluorescence in 200 µL of rinse-water or meltwater
172 using a BioTurner 20/20n Luminometer (P/N 2030-002) equipped with the blue
173 fluorescence module (BioTurner 2030-041). The pETBlue-2 plasmid component was
174 monitored using a PCR with the following conditions: 1 U of Taq DNA polymerase
175 (5PRIME), 1× MasterTaq buffer, 1× TaqMaster PCR enhancer, 1.5 mM Mg^{2+}, 0.2 µM of each
176 primer (TF7: 5'-TAATACGACTCACTATAGGG -3'; pETBlue-DOWN: 5'-
177 GTTAAATTGCTAACGCAGTCA-3'), 200 µM dNTPs, and ~100 pg of template DNA. Thirty
178 cycles of PCR were done with a 30 s denaturation step at 94 °C, 60 s annealing step at 55 °C
179 and extension at 72 °C for 60 s, followed by a final extension at 72 °C for 10 min. The
180 presence of viable *E. coli* was monitored by spread plating rinse-water and meltwater on
181 agar-solidified LB media containing ampicillin (100 µg mL^{-1}) followed by incubation at 37
182 °C. Samples in which any component of the tracer solution was detected in the final
183 meltwater were discarded and reprocessed from a new subsample.

184 **2.3 ATP analysis**

185 Immediately after melting, samples were filtered through 0.22 μm pore size
186 polyethersulfone (Supor; Pall) filters using a bench-top vacuum manifold (≤ 20 kPa). Clean
187 ice samples were filtered through a 25 mm diameter filter while banded, solid, and
188 dispersed ice samples were processed through either a 47 mm or 90 mm diameter filter,
189 depending on total sediment content. The filters were cut into small pieces using a sterile
190 scalpel and extracted on a vortex mixer for 10 seconds with 5 mL of boiling Tris-acetate
191 buffer (TAB; 50mM Tris base adjusted to pH 7.75 with acetic acid). The filters were then
192 incubated in a boiling water bath for 5 minutes and immediately placed on ice for 30
193 minutes. Extracts were centrifuged for 5 minutes at 4500×g to remove debris and the
194 supernatant was collected.

195 The concentration of ATP was measured in the extracts using a modification of the
196 firefly luciferase-luciferin assay described by (Amato and Christner, 2009). Briefly, 10 μL of
197 extract was added to an equal volume of triethanolamine buffer (TEOA buffer; 200 mM
198 triethanolamine pH 7.6, 2 mM MgCl2, 240 mM KCL) and incubated at 37°C for 10 minutes.
199 To correct for adenylate adsorption to and luciferase inhibition by the sediment in the
200 sample extracts, two samples were prepared in parallel for each measurement. Following
201 incubation at 37°C, 10 uL of TAB supplemented with 10 μM ATP was added to one of the
202 samples to serve as an internal standard for each measurement. All samples were kept on
203 ice during preparation but were equilibrated to room temperature (22 °C) prior to the
204 addition of luciferase and measurement of luminescence.

205 Weighted linear regression was used to generate calibration curves using
206 concentrations of ATP (in TAB) from 10 μM to 1 pM. The luciferase-luciferin cocktail was

207 prepared fresh for each series of measurements and consisted of 100 U ml^{-1} luciferase and
208 0.140 mM D-luciferin. Luminescence was quantified with a 20/20n luminometer
209 (Promega) using auto-injection of 100 µL of the luciferase-luciferin cocktail. Relative
210 luminescence units (RLU) were integrated for three seconds immediately after injection.
211 Sample RLU values were corrected for adsorption and inhibition using the following
212 formula:

213 $$\frac{1}{\left(\frac{RLU_{\text{sample+std}} - RLU_{\text{sample}}}{RLU_{\text{blank+std}}}\right)} \times RLU_{\text{sample}} = RLU_{\text{corrected}}$$

214

215 The corrected RLU values were used together with the standard calibration curve to
216 determine the ATP concentration in the extractant. Final ATP concentrations were
217 corrected for dilution and normalized to the mass of the ice sampled. All values reported
218 are the means of replicate samples (n = 3 to 5).

219 **2.4 Nucleic acid extraction**

220 After decontamination, basal ice samples were placed in a sterilized container, and
221 melted at 4°C. For samples from sediment-rich basal ice (i.e. banded, solid, and dispersed
222 ice), DNA was extracted directly from the sediment recovered after melting using MoBio
223 PowerMax DNA Isolation kits. To increase DNA extraction yields, two 10g (wet weight)
224 extractions were combined onto a single silica spin column for each sample. For samples
225 from sediment-poor basal ice (i.e. clean ice), meltwater was filtered onto 47 mm, 0.22 µm
226 pore size Supor PES filter membranes (Pall) with ≤20 cm Hg of vacuum. DNA was extracted
227 from the filters using MoBio PowerWater DNA Isolation kits as per the manufacturer's
228 instructions with one exception: the mechanical lysis step was performed on a BioSpec

229 MiniBeadbeater-8 for 2 minutes at maximum speed. All DNA samples were stored at -80°C
230 until PCR amplification.
231 Due to the low biomass we expected in the basal ice (≤10^4 cells g^{-1}; (Doyle *et al.*,
232 2013)), very large samples (~5 kg of ice) were processed to recover enough RNA for
233 reverse transcription PCR (Table S1). To facilitate filtration of such large sample sizes,
234 coarse sediment was removed from sediment-rich basal ice samples after melting using
235 low speed centrifugation (700×g, 10 min, 4°C). The resulting supernatant containing fine
236 clay and silt-like particles was then concentrated onto 90 mm, 0.22 µm pore size Supor PES
237 filter membranes. Meltwater from clean ice samples did not require this centrifugation step
238 and were directly filtered onto 90mm, 0.22 µm pore size Supor PES filters. After filtration,
239 all filters were immediately processed for RNA extraction using a modified phenol-
240 chloroform extraction protocol (Dieser *et al.*, 2014). Briefly, filters were sliced into small
241 pieces using a sterile scalpel, immersed in 3 mL of TE buffer (1 mM EDTA, 10 mM Tris; pH
242 6.3) containing lysozyme (15 mg mL^{-1}), and vortexed for 30 minutes at room temperature.
243 Samples were then homogenized in a BioSpec Mini-Beadbeater for 2 minutes at maximum
244 speed using ~1 g of sterilized 0.1 mm diameter zirconia/silica beads. After bead beating,
245 crude extracts were amended with two volumes of chilled (4°C) denaturing buffer (4M
246 guanidine thiocyanate, 50 mM Tris, 10 mM EDTA, 1% w/v N-lauroylsarcosine, 1% β-
247 mercaptoethanol), the resulting insoluble material was pelleted via centrifugation (4500×g
248 for 5 min at 4°C), and the supernatant was collected. The pellet was washed with 3 mL of
249 chilled denaturing buffer, centrifuged again, and the resulting supernatant pooled with the
250 first. This pooled lysate was then extracted with an equal volume of
251 phenol:chloroform:isoamyl alcohol (25:24:1, pH 6.6), followed by a second extraction with

252 chloroform:isoamyl alcohol (24:1). Nucleic acids were purified from these extracts via an
253 overnight ethanol precipitation with 0.3 M sodium acetate (pH 6.0). Linear acrylamide (20
254 μg mL^{-1}; Ambion) was used as a coprecipitant to aid recovery. Genomic DNA was
255 eliminated from RNA extracts by digesting for one hour at 37°C with 4 U of TURBO DNAase
256 (Ambion) followed by purification with MEGAclear Transcription Clean-Up kits (Ambion).
257 Extracted DNA and RNA concentrations were measured using Quant-it Picogreen and
258 Ribogreen kits (Life Technologies), respectively, per the manufacturer's instructions.

259 **2.5 16S rRNA amplicon sequencing**

260 From the RNA extracted, complementary DNA (cDNA) was reverse transcribed from
261 ~1 ng of total RNA using SuperScript II reverse transcriptase with the 806R primer (5'-
262 GGACTACVSGGGTATCTAAT-3') following the manufacturer's protocol. Negative control
263 reactions lacking RNA template or reverse transcriptase were conducted to monitor for
264 contaminating RNA and DNA molecules, respectively.

265 The hyper-variable V4 region of the 16S rRNA gene was PCR amplified from the
266 DNA extracts and cDNA libraries using a barcoded 515F-806R primer pair (Caporaso *et al.*,
267 2012). Each 50 μL PCR contained ~100 pg of DNA or cDNA, 2.5 U of AmpliTaq Gold DNA
268 polymerase LD (Invitrogen), 1× Gold Buffer, 2.5 mM $MgCl_2$, 0.2 μM of each primer, and 0.2
269 μM dNTPs. Amplification conditions included at 95°C for 9 min, followed by 30 to 40 cycles
270 of denaturation at 94°C for 1 min, annealing at 50°C for 30 s, and extension at 72°C for 30 s.
271 A final extension was performed at 72°C for 10 min. Following amplification, amplicons
272 were separated by electrophoresis on a 2% agarose gel to assess relative band intensity
273 and size. The amplicons were quantified with Quant-it fluorometry and pooled at
274 equimolar concentrations. Two extraction blanks were included in the pooled libraries to

275 serve as procedural controls (Salter *et al.*, 2014). Pooled libraries were purified with a
276 MoBio UltraClean PCR Cleanup Kit and sequenced on the Illumina MiSeq platform (v2
277 chemistry, 2× 250 bp; Georgia Genomics Facility).

278 **2.6 16S rRNA amplicon analysis**

279 Sequence read curation and processing was performed using DADA2 (Callahan *et*
280 *al.*, 2016) with the following filtering parameters (maxN=0, trunQ=2, rm.phix=TRUE,
281 maxEE=2, R1 truncLen=240, R2 truncLen=200). Error rates for the filtered and trimmed
282 R1 and R2 reads were calculated using the *learnErrors* function and subsequently used to
283 denoise reads using the DADA2 sample inference algorithm. The denoised reads were
284 merged into amplicon sequence variants (ASV) using a global ends-free alignment. Paired
285 reads containing mismatches in the overlapping region were removed from the dataset.
286 Chimeric ASVs were identified and removed by using the consensus method within the
287 *removeBimeraDenovo* function. A consensus taxonomy for each ASV was then assigned
288 using a naïve Bayesian classifier (Wang *et al.*, 2007) trained on release 132 of the SILVA
289 reference database (Quast *et al.*, 2013). The dataset was then subsampled to an even read
290 depth across all samples (59,577 sequences). Any ASV classified as a chloroplast,
291 mitochondria, or from which ≥0.1% of its reads were from a procedural blank were
292 removed. Any ASV that was observed exclusively in an RNA library was flagged as a
293 potential contaminant.

294 **2.7 Meta-analyses of microbiomes of permanently frozen ecosystems**

295 Publicly available 16S rRNA amplicon datasets from similar permanently frozen
296 environments were identified using a search of the NCBI Sequence Read Archive and
297 downloaded using the SRA Toolbox *fastq-dump* function. Run tables were aggregated and

298 studies based on Sanger sequencing were excluded; only datasets based on Illumina, 454,
299 or IonTorrent sequencing were considered in the analysis. Datasets wherein the sequence
300 reads were not demultiplexed before being uploaded to the SRA were also excluded. A list
301 of datasets that met these criteria and were included in the meta-analysis are detailed in
302 Table S2.

303 Each dataset was individually processed using DADA2 to infer ASV sequences and
304 produce an ASV table. For each study, the filtering parameters were adjusted to account for
305 variation in fragment length and the 16S rRNA variable region sequenced. Due to higher
306 rates of homopolymer and indel errors with 454 and IonTorrent sequencing, datasets using
307 these platforms used a band size parameter of 32 and homopolymer region (≥ 3 repeated
308 bases) gap cost of -1 during the sample inference algorithm. For Illumina datasets, the band
309 size parameter was set to 16 and gaps in homopolymer regions were treated as normal
310 gaps (gap cost of -8). Nine datasets had to be removed from the meta-analysis after these
311 steps due to the loss of too many sequences during quality control steps within the DADA2
312 pipeline. Complete parameter details and throughput statistics for each dataset in the final
313 meta-analysis are available in Table S3 and S4.

314 ASV sequences from each study were merged and inserted into the 99% Greengenes
315 reference tree (McDonald *et al.*, 2012) using the SATé-enabled phylogenetic placement
316 (SEPP) technique (Mirarab *et al.*, 2012) within the QIIME2 *fragment-insertion* plugin
317 (Janssen *et al.*, 2018). The merged ASV tables from each study were filtered to remove ASVs
318 rejected from tree insertion by SEPP.

319

320

321 **2.8 Data availability**

322 Sequence read data generated in this study is available on NCBI SRA under
323 BioProject PRJNA282540.

324

325 **3. RESULTS**

326 **3.1 Description of Basal Ice Samples**

327 Based on the nomenclature of (Hubbard *et al.*, 2009), we identified three distinct
328 types of basal ice in the basal ice profiles sampled from Taylor Glacier: clean ice, banded
329 ice, and solid ice (Table 1; Figure S3). All three types were collected during the 2007
330 expedition, while only clean ice and banded ice horizons were targeted during the 2009
331 expedition. The basal ice recovered from Matanuska Glacier was identified as dispersed ice
332 and was the only type observed at the location of sampling.

Table 1. Description of basal ice types collected in this study

Type	Glacier	Temp (°C)	Description
Clean ice	Taylor	-15	debris-free ice
Banded ice	Taylor	-15	finely stratified layers of debris and ice, layers range in thickness from a few mm to several cm
Solid ice	Taylor	-15	composed primarily of frozen debris with only interstitial ice, no visible layering
Dispersed ice	Matanuska	~0	contains scattered debris aggregated into small clusters, no visible layering

333

334 **3.2 Nucleic acids in sediment-rich and sediment-poor basal ice**

335 The amount of DNA and RNA extracted from each sample was normalized to sample
336 mass to assess the relative amounts of microbial biomass present within each type of basal
337 ice. Using this approach, we measured approximately 10,000-fold more DNA per gram of
338 basal ice in the sediment-rich basal ice types (i.e. banded, solid, and dispersed) than in the

339 sediment-poor clean ice (Table 2). Between the sediment-rich basal ice types, the
340 temperate dispersed basal ice from Matanuska Glacier contained approximately 6-fold
341 more DNA per gram of ice than the banded and solid basal ices from the cold-based (-15°C)
342 Taylor Glacier. RNA concentrations were very low in all basal ice types, with the highest
343 concentration—though only marginally—observed in Matanuska's dispersed basal ice.

Table 2. Cell counts, biomass estimates, and yield of DNA and RNA extracted from basal ice samples. Sediment-rich basal ice facies are highlighted in gray.

	Cell Counts*	Yield (pg g^{-1} ice)		Biomass Estimates	
Sample	cells g^{-1} ice ($\times 10^3$)	DNA	RNA	estimated genomes† g^{-1} ice ($\times 10^3$)	ATP (pg g^{-1} ice)
Clean07	0.3 - 0.5	4.7	0.7	1.9	<0.01 - 0.04
Clean09	-	1.4	-	0.6	-
Banded07	1.8 - 18.2	16994.3	2.3	6797.7	-
Banded09	-	16140.1	0.8	6456.0	0.24 - 2.8
Solid	6.7	14366.2	1.2	5746.5	<0.01
Dispersed	-	98860.2	3.2	39544.1	0.06 - 0.14

344 *Doyle et al. 2014. †Estimated number of microbial genomes estimated using 2.5 fg of DNA per genome

345 **3.3 Composition of microbial assemblages in different types of basal ice**

346 A total of 4,227,678 paired-end reads with an average read length of 253bp were
347 obtained from MiSeq sequencing. After filtration and denoising, 2,883,221 non-chimeric
348 sequences representing 3310 ASVs remained. Subsampling and culling of ASVs classified as
349 plastids or flagged as potential contaminants produced a final, curated dataset composed of
350 2021 ASVs. Based on average-neighbor clustering of Bray-Curtis distances, the basal ice
351 samples clustered into three significantly different (AMOVA; $F[2,3]=5.23$, $p=0.017$) groups:
352 (1) Taylor Glacier sediment-poor basal ice, (2) Taylor Glacier sediment-rich basal ice, and
353 (3) Matanuska Glacier dispersed ice. The sediment-poor clean ice samples contained

354 microbial assemblages overwhelmingly composed of *Firmicutes* (68%) and *Proteobacteria*
355 (25%), with smaller proportions of *Bacteroidetes* (5%) and *Actinobacteria* (1%). The genus
356 *Tumebacillus* was especially abundant in the clean ice samples (Figure 1A). Assemblages
357 within the banded and solid ice samples were comparatively more diverse than those
358 found in clean ice (Figure 2), with a wider range of abundant phyla represented:
359 *Actinobacteria* (26%), *Firmicutes* (23%), *Bacteroidetes* (19%), *Proteobacteria* (11%),
360 *Atribacteria* (9%), *Tenericutes* (7%), and *Planctomycetes* (1%). Notably, ASVs related to the
361 class *Clostridia* composed about 20% of the communities in these samples. Lastly, the
362 microbial assemblage within Matanuska's dispersed basal ice was distinct from those
363 observed from Taylor Glacier. Here we observed significant amounts of *Nitrospirae* (39%)
364 and *Betaproteobacteria* (30%), of which several of the most abundant ASVs were related to
365 sulfur and/or iron cycling members of the genera *Thermodesulfovibrio*, *Rhodoferax*, and
366 *Thiobacillus*.

367 **3.4 Assessing metabolic status of bacterial taxa within different types of basal ice**

368 With the RNA libraries, we identified 141 potentially metabolically active ASVs (7%
369 of total) taxa within the basal ice. Of these ASVs, 80 had RNA/DNA abundance log-ratios >1
370 (Table S5) and thus we focused on these as having the highest potential for metabolic
371 activity. The vast majority (63 ASVs) of these taxa were observed in the dispersed ice from
372 Matanuska Glacier (Figure 1B), the warmest and youngest basal ice sampled in this study.
373 Here, many of these ASVs were members of the *Chloroflexi* or *Deltaproteobacteria,* with
374 some of the largest RNA/DNA abundance log-ratios belonging to *Desulfocapsa*, *Syntrophus*,
375 and unassigned members of the family *Anaerolineaceae*. Within the banded basal ice from
376 Taylor Glacier, over half of potentially active ASVs instead belonged to the *Firmicutes*.

377 Among this phylum, members of the *Paenisporosarcina*, *Paenibacillaceae*,
378 *Desulfosporosinus*, *Caldicoprobacter*, and *Virgibacillus* had by far the highest activity
379 potential and represented >90% of the RNA reads in these samples. In comparison, the
380 clean and solid basal ice had the least number of potentially active ASVs—10 altogether
381 comprising only 472 RNA reads in total, only 2 of which had RNA/DNA abundance log-
382 ratios >1—suggesting very little to no metabolic activity.

383 **3.5 Meta-Analysis: Microbial populations of various permanently frozen**
384 **environments**

385 For the meta-analysis, we analyzed 33.6 million 16S rRNA sequences across 146
386 individual samples from 15 publicly available datasets that represented five different types
387 of permanently frozen environments: (1) supraglacial ice, (2) englacial ice, (3) basal ice, (4)
388 perennial cave ice, and (6) permafrost. After filtering and curation, the final meta-analysis
389 dataset contained 17.5 million non-chimeric sequences representing 14,114 unique ASVs.

390 We calculated Shannon Diversity indices to compare microbial alpha diversity
391 between these frozen environments. Of the basal ice assemblages characterized in this
392 study, alpha diversity was higher in sediment-rich basal ice types than in the sediment-
393 poor clean ice ($t(4)=3.34$, $p=0.03$) (Figure 2). Compared to the other frozen environments
394 in this meta-analysis, alpha diversity within our sediment-rich basal ice samples from
395 Antarctica were most similar to that observed in permafrost sampled from the Storflaket
396 peat bog in northern Sweden (Monteux *et al.*, 2018). Conversely, alpha diversity within
397 Taylor Glacier's clean ice was most similar to that found in englacial ice samples from the
398 GISP2D, NEEM, and WAIS Divide ice cores (Buford Price *et al.*, 2015).

399 To visualize microbial β-diversity between samples, we used a hierarchical cluster
400 analysis of weighted UniFrac distances (wUF). Microbial communities largely clustered by
401 the type of permanently frozen environment they inhabited, though some environments
402 displayed larger variation in community structures than others. For example, communities
403 inhabiting englacial ice were the most similar (wUF: 0.47 ± 0.15; mean ± s.d). In contrast,
404 perennial cave ice samples from a single location (Itcus *et al.*, 2018) harbored the widest
405 range of microbial communities (wUf: 0.81 ± 0.14). β-diversity of permafrost microbiomes
406 were more intermediate: relatively tight clustering was observed in permafrost from the
407 Storflaket peat bog (northern Sweden) with wider variation in samples of permafrost from
408 University Valley (Antarctica) (Goordial *et al.*, 2016; Monteux *et al.*, 2018). The microbial
409 communities within the Taylor Glacier's banded and solid basal ice facies clustered closely
410 with the Sweden permafrost samples, while those within the clean basal ice and
411 Matanuska's dispersed basal ice were most similar to those observed in englacial ice from
412 the NEEM ice core in Greenland (Miteva *et al.*, 2015, 2016)(Figure 3).
413 We used an RDA model to determine how microbial lineages were distributed
414 across the different types of frozen environments (Figure 4, left). The final RDA model
415 explained 24.9% of the variability between samples and effectively separated the samples
416 into three clusters, like that seen in Figure 3. Of the 89 microbial lineages included in this
417 analysis, we identified 14 had loading vectors greater than the equilibrium contribution—
418 the proportion of variance which would be explained by a random constrained axis—
419 indicating they were differentially abundant across the five types of frozen environments.
420 Scalar projections of these lineages onto the centroid factor of each type of frozen
421 environment allowed us to estimate how strongly these lineages were associated with each

422 environment (Figure 4, right). As one would expect, supraglacial ice environments
423 harbored comparatively higher proportions of *Cyanobacteria* and plastid-related taxa than
424 the other frozen environments. Englacial ice environments were instead enriched with
425 members of the *Pseudomonas*, *Janthinobacterium*, *Methylobacterium*, and *Oxalobacteraceae*.
426 In contrast, basal ice, permafrost, and perennial cave ice environments all contained higher
427 populations *Firmicutes* related lineages: *Clostridium*, *Ruminococcaceae*, *Desulfosporosinus*,
428 and *Paenibacillus*.
429

430 **4. DISCUSSION**

431 **4.1 Microbial communities vary in size and composition across basal ice types**

432 Of the four different types of basal ice analyzed in this study, we found that those
433 containing large quantities of sediment or debris contained more extractable nucleic acids,
434 consistent with higher microbial abundances than those containing little or no subglacial
435 sediments. This is consistent with previous microscopic investigations of the GISP2 ice core
436 that found higher cell concentrations in deeper sections of the core where clay particles
437 were embedded in the ice (Tung *et al.*, 2006). In addition to higher numbers of cells and
438 biomass, microbial diversity was also notably higher in the sediment-rich basal ice facies
439 relative to clean basal ice or englacial ice, indicating that subglacial debris is the primary
440 source of microorganisms in the basal ice.

441 Our estimates of bacterial cell abundance based on extracted DNA yields (~10^6 cells
442 g^{-1} ice) were approximately 100-fold higher than those based on direct microscopic counts
443 (~10^4 cells g^{-1} ice), but only in the sediment-rich banded and solid basal ice. In the clean

basal ice, these estimates were comparable. This suggests that Taylor Glacier's debris-rich basal ice may contain significant amounts of microbial necromass.

We found microbial assemblages within basal ices of the cold-based (-15°C) Taylor Glacier contain high abundances of *Firmicutes* and *Actinobacteria* relative to the other frozen habitats examined. Bacteria within these two phyla have been commonly observed as the dominant taxa in a wide-range of frozen environments such as ground ice, permafrost, polar saline springs, cryopegs, and sea ice (Kochkina *et al.*, 2001; Steven *et al.*, 2007, 2008; Perreault *et al.*, 2008; Lacelle *et al.*, 2011; Boetius *et al.*, 2015; Spirina *et al.*, 2017). One explanation for these observations is that the physiochemical stresses faced by cells under frozen conditions (Doyle *et al.*, 2012) favor the prevalence of microorganisms that can form highly resistant endospores (*Firmicutes*) or spores (*Actinobacteria*). Although this is consistent with the notion that extreme environmental conditions select for microbial lineages with robust survival strategies (Filippidou *et al.*, 2016), multiple lines of evidence indicate this hypothesis does not adequately explain the abundance of these taxa in our basal ice samples. First, ASVs related to known endospore-forming genera such as *Paenisporosarcina*, *Virgibacillus*, *Clostridium*, and *Desulfosporosinus* were abundant in all our RNA libraries. Because the rRNA content of endospores decreases relatively quickly after sporulation—on the order of days to weeks (Segev *et al.*, 2012; Korza *et al.*, 2016)—their detection in ≥10,000 year-old basal ice strongly implies these taxa existed as vegetative cells within the ice. Second, we found cultured isolates of *Paenisporosarcina* sp. recovered directly from Taylor Glacier banded ice would not sporulate after being refrozen in basal meltwater at in situ temperatures (-15°C), but instead continuously incorporate radiolabeled substrates into macromolecules (Doyle *et al.*, 2013). Third, these isolates were

heat-killed if the banded basal ice meltwater was pasteurized prior to cultivation experiments, indicating we were not recovering these isolates from ancient endospores. Finally, these findings are consistent with recent a study that performed 16S rRNA gene sequencing of ancient permafrost samples after endospore enrichment and selective depletion of DNA from dead cells and found many bacteria capable of forming endospores, especially members of the *Clostridia*, were in a nondormant state (Burkert *et al.*, 2019). Collectively, these results suggest the high abundances of *Firmicutes* and *Actinobacteria* in Taylor Glacier's basal ice is because they had the ability to remain active while frozen as opposed to simply enduring in a durable, yet dormant state.

4.2 Young and warm versus old and cold basal ice

Due to the chemical lability of RNA, paired RNA/DNA 16S rRNA amplicon libraries are a useful tool for discerning live organisms in a microbial community from those that are long-dead or dormant. One should note there are limitations to this analysis and these ratios are more reliable indicators of potential activity rather than real-time activity (Blazewicz *et al.*, 2013).

On average, only about 2% of the total ASVs in each sample were also detected in the paired RNA library. This low proportion of potentially active ASVs suggests only a small fraction of the microorganisms entrained into basal ice are suited to remain metabolically active inside ice. Despite this small fraction, a pattern does emerge: the dispersed basal ice from Matanuska Glacier contained a much larger population of potentially active ASVs than any of the basal ice cryofacies recovered from Taylor Glacier.

One plausible explanation for this observation is the substantial difference in geology and age of basal ice between these two glaciers. Assuming a non-zero rate of

microbial attrition over time in ice due to, for example, the accumulation of cellular damage or the depletion of resources, older ice would be expected to harbor smaller populations of potentially active microorganisms than younger ice. Analysis of the δD and $\delta^{18}O$ composition of meltwater from Taylor Glacier surface ice samples estimated they are between 11,500 and 65,000 years old (Aciego *et al.*, 2007), while more recent radiometric ^{81}Kr dating efforts near the glacial terminus expanded this estimate to nearly 123,500 years old (Buizert *et al.*, 2014). In comparison, measurements of oxygen isotopes in Matanuska Glacier's dispersed basal ice layer indicated the basal ice originated in the accumulation area (Lawson and Kulla, 1978). Based on the velocity of Matanuska Glacier (~110 m yr^{-1}), this would represent an approximate time of 250 years between deposition and terminal ablation. Trace amounts of anthropogenic tritium produced by atmospheric thermonuclear weapon tests in the 1950s and 1960s have also been detected in Matanuska Glacier's basal ice zone (Strasser *et al.*, 1996), indicating portions of this ice were formed even more recently by subglacial freeze-on of surface-derived meltwater (Lawson, 1979). Taken together, this indicates the dispersed ice we sampled from Matanuska is substantially younger than any of the basal ice types we collected from Taylor Glacier.

In addition to ice age, the large difference in ice temperature between a temperate and cold-based glacier should also affect the potential for metabolic activity in basal ice environments. Taylor Glacier is primarily a cold-based glacier with a measured basal ice temperature of -15°C (Montross *et al.*, 2014). In contrast, Matanuska Glacier is a temperate glacier with a basal ice zone temperature just below 0°C (Lawson *et al.*, 1998). As such, cells frozen in Taylor Glacier's basal ice are under considerably higher physiochemical stress than ice near the melting point. For example, the predicted ionic strength of the

513 briny liquid at ice crystal boundaries—where the microorganisms also exist— is nearly
514 4.6M at -15°C. Comparatively, this is 11.5-fold higher than the unfrozen water in ice at -1°C
515 (Doyle *et al.*, 2012). Hence, the wider diversity and increased number of ASVs with a high
516 potential for metabolic activity in the dispersed basal ice may reflect the more favorable
517 conditions for metabolism in temperate versus cold-based glacial ice.

518 **4.3 Debris-rich basal ice types are hot spots for microbial activity**

519 Previous analyses of the gasses entrapped within Taylor Glacier banded basal ice
520 found that that O_2 was depleted to as low as 4% in horizons where CO_2 concentrations
521 were concurrently enriched as high as 20,000-fold relative to atmospheric concentrations
522 (Montross *et al.*, 2014). Isotopic analyses of $\delta^{13}C$-CO_2 revealed this CO_2 is isotopically
523 depleted (-24‰), and therefore, was likely produced by *in situ* microbial respiration of
524 organic matter (Montross, 2012). This data supports our RNA-based 16S rRNA analyses,
525 which found the largest read counts and number of potentially active ASVs in the same
526 banded basal ice samples. Together, these observations strongly suggest Taylor Glacier's
527 banded basal ice horizons harbor metabolically active microbiomes that are altering the ice
528 gas chemistry at temperature of -15°C.

529 We also observed an enrichment of anaerobic taxa (e.g. *Clostridia*) within the same
530 banded basal ice samples where O_2 concentrations were depleted. This raises the intriguing
531 possibility that, given sufficient time, the microbiomes of debris-rich basal ice may shift to
532 members with anoxic and anaerobic metabolisms (e.g. methanogenesis). In support of this,
533 multiple investigations have found large excesses of CH_4 in debris-rich basal ice samples
534 from Greenland and Antarctica (Tung *et al.*, 2006; Stibal *et al.*, 2012; Wadham *et al.*, 2012;
535 Rhodes *et al.*, 2013; Lamarche-Gagnon *et al.*, 2019; Lee *et al.*, 2020). This hypothesis is also

supported by a recent laboratory experiment that suggests cryoconite hole meltwater will become enriched with anaerobic taxa after it is transported to a subglacial environment (Zdanowski *et al.*, 2017). However, it should be noted that this study was not performed in ice.

Previous chemical analysis of Taylor Glacier's basal ice revealed dissolved organic carbon (DOC) concentrations are much higher in the debris-rich basal ice types (~63 mg L^{-1}) than in the debris-poor types (~0.8 mg L^{-1})(Montross, 2012; Montross *et al.*, 2014). This is also consistent with our microbiological results. Increased microbial activity in debris-rich basal ice horizons may simply be a consequence of there being more substrates available to consume. However, our investigation of multiple basal ice types indicates there are likely additional, unidentified factors besides sediment content controlling whether basal ice harbors an active microbiome. For example, although the banded and solid basal ice samples harbored very similar microbial communities in our DNA-based libraries, we found very little evidence for active ASVs within the solid basal ice. This suggests—at least in polar glaciers containing basal ice horizons well below 0°C—the presence of debris and/or DOC alone is not sufficient to support a metabolically active microbiome.

4.4. Phylogenetically similar communities in debris-rich basal ice and permafrost

Our meta-analysis indicates that that microbial communities within the banded and solid basal ice from Taylor Glacier were phylogenetically most like those in permafrost and were more distantly related to those in englacial ices and supraglacial ecosystems. This suggests the ecophysiological stresses experienced by cells frozen in permafrost and basal ice of a cold-based glacier are comparable and select for similar taxa. Both subsurface environments contain high mineral debris and may remain frozen for many thousands of

559 years. In fact, there is debate on whether the physical differences between cold, debris-rich
560 basal ice and permafrost are only terminological (Dobinski, 2006; Dąbski, 2019). Our
561 results support this contention, adding a microbiological dimension that provides
562 additional evidence for the parallels between these cryospheric environments. New data
563 from other cold-based glaciers and regions are needed to test if these similarities in
564 microbial composition with permafrost are robust across multiple locales. If so, permafrost
565 environments may be a useful analog for gaining valuable insight into the microbiology of
566 unexplored basal ice environments which are logistically more difficult to access.

567 **4.5 Meta-analysis limitations**

568 Comparing 16S amplicon datasets from different studies is often hindered by
569 inconsistencies in sequencing platform used and which variable region of the 16S rRNA
570 gene was amplified. Using SEPP to insert heterogeneous ASVs from different studies into
571 the same reference tree creates stable phylogenetic placements, enabling integration and
572 meta-analysis of amplicon data from multiple variable regions of the 16S rRNA gene
573 (Janssen *et al.*, 2018). Despite this, it is important to note the limitations of this approach.
574 First, integrating previously published 16S rRNA amplicon datasets based on Sanger
575 sequencing of clone libraries or DGGE profiling remains difficult as these older approaches
576 lack the read depth or taxonomic resolution to make meaningful comparisons with those
577 datasets prepared with more modern approaches. As a result, our meta-analysis
578 unfortunately excluded many early works which investigated the microbial ecology of
579 glacial ice using these approaches. Second, there are some potential biases in our meta-
580 analysis due to low coverage: despite growing interest in the microbial ecology of the
581 cryosphere, high-throughput surveys of permanently frozen ecosystems are still

uncommon. For example, the Matanuska dispersed basal ice most resembled englacial ice samples in our meta-analysis. However, many of the englacial ice samples in the meta-analysis are also from Matanuska Glacier. Indeed, there are exceedingly few microbiome analyses of true englacial ice samples unaffected by either supraglacial or subglacial processes, largely due to both the logistical difficulty of accessing and sampling these environments.

4.6 Conclusions and Implications

Our findings show that certain microbes do not persist in a state of dormancy while frozen and, coupled with other biogeochemical data (Doyle *et al.*, 2013; Montross *et al.*, 2014), indicate that some sediment-rich basal ice horizons host active microbial communities that participate in biogeochemical cycling. Although we have limited observations, our data further implies that a larger diversity of bacteria may remain metabolically active in the relatively warm basal ice found beneath temperate glaciers and ice sheet interiors (Lawson *et al.*, 1998; Bell *et al.*, 2011). Indeed, since the basal temperature of the Antarctic and Greenland ice sheets are near or at the pressure-melting point (Gow *et al.*, 1968), this raises the intriguing possibility that these regions of the cryosphere are more biogeochemically active than previously thought. We also found that microorganisms in the basal ice of cold-based glaciers may be important biogeochemical actors as well. Although rates of microbial activity in these environments are certainly slower than those of warmer environments (Christner, 2002; Panikov *et al.*, 2006; Amato *et al.*, 2009, 2010; Doyle *et al.*, 2013), this may be offset by the long residence time of most basal ice environments, providing ample time for biogeochemical processing. As climate change continues to shrink the cryosphere and warm more basal ice environments, this

605 may be an important consideration for high latitude land- and marine-based coastal
606 environments that receive regular discharges of meltwater derived from ancient basal ice
607 horizons, an important source of dissolved organic carbon, nutrients, and trace metals
608 (Rignot and Jacobs, 2002; Jung *et al.*, 2019; Vick-Majors *et al.*, 2020).
609

610 **5. ACKNOWLEDGEMENTS**

611 This study was funded by a Division of Polar Programs grant (ANT-0636828) from
612 the National Science Foundation.
613

614 **6. REFERENCES**

615 Aciego, S.M., Cuffey, K.M., Kavanaugh, J.L., Morse, D.L., and Severinghaus, J.P. (2007)
616 Pleistocene ice and paleo-strain rates at Taylor Glacier, Antarctica. *Quaternary*
617 *Research* **68**: 303–313.
618 Amato, P. and Christner, B.C. (2009) Energy Metabolism Response to Low-Temperature
619 and Frozen Conditions in Psychrobacter cryohalolentis. *Applied and Environmental*
620 *Microbiology* **75**: 711–718.
621 Amato, P., Doyle, S., and Christner, B.C. (2009) Macromolecular synthesis by yeasts under
622 frozen conditions. *Environmental Microbiology* **11**: 589–596.
623 Amato, P., Doyle, S.M., Battista, J.R., and Christner, B.C. (2010) Implications of Subzero
624 Metabolic Activity on Long-Term Microbial Survival in Terrestrial and
625 Extraterrestrial Permafrost. *Astrobiology* **10**: 789–798.
626 Barker, J.D., Grottoli, A.G., and Lyons, W.B. (2018) Stable isotope evidence for the
627 biogeochemical transformation of ancient organic matter beneath Suess Glacier,
628 Antarctica. *Arctic, Antarctic, and Alpine Research* **50**: e1448643.
629 Batjes, N.H. (2014) Total carbon and nitrogen in the soils of the world. *European Journal of*
630 *Soil Science* **65**: 10–21.
631 Bell, R.E., Ferraccioli, F., Creyts, T.T., Braaten, D., Corr, H., Das, I., et al. (2011) Widespread
632 Persistent Thickening of the East Antarctic Ice Sheet by Freezing from the Base.
633 *Science* **331**: 1592–1595.
634 Bhatia, M.P., Das, S.B., Xu, L., Charette, M.A., Wadham, J.L., and Kujawinski, E.B. (2013)
635 Organic carbon export from the Greenland ice sheet. *Geochimica et Cosmochimica*
636 *Acta* **109**: 329–344.
637 Blazewicz, S.J., Barnard, R.L., Daly, R.A., and Firestone, M.K. (2013) Evaluating rRNA as an
638 indicator of microbial activity in environmental communities: limitations and uses.
639 *The ISME Journal* **7**: 2061–2068.

Boetius, A., Anesio, A.M., Deming, J.W., Mikucki, J.A., and Rapp, J.Z. (2015) Microbial ecology of the cryosphere: sea ice and glacial habitats. *Nature Reviews Microbiology* **13**: 677–690.

Boyd, E.S., Skidmore, M., Mitchell, A.C., Bakermans, C., and Peters, J.W. (2010) Methanogenesis in subglacial sediments: Subglacial methanogenesis. *Environmental Microbiology Reports* **2**: 685–692.

Buford Price, P., Jeffrey Morris, J., Bay, R.C., Adhikari, A., Giovannoni, S.J., and Vergin, K.L. (2015) Molecular Fossils from Microorganisms Preserved in Glacial Ice. *bioRxiv*.

Buizert, C., Baggenstos, D., Jiang, W., Purtschert, R., Petrenko, V.V., Lu, Z.-T., et al. (2014) Radiometric 81Kr dating identifies 120,000-year-old ice at Taylor Glacier, Antarctica. *Proceedings of the National Academy of Sciences* **111**: 6876–6881.

Burkert, A., Douglas, T.A., Waldrop, M.P., and Mackelprang, R. (2019) Changes in the Active, Dead, and Dormant Microbial Community Structure across a Pleistocene Permafrost Chronosequence. *Appl Environ Microbiol* **85**: e02646-18.

Callahan, B.J., McMurdie, P.J., Rosen, M.J., Han, A.W., Johnson, A.J.A., and Holmes, S.P. (2016) DADA2: High-resolution sample inference from Illumina amplicon data. *Nature Methods* **13**: 581–583.

Caporaso, J.G., Lauber, C.L., Walters, W.A., Berg-Lyons, D., Huntley, J., Fierer, N., et al. (2012) Ultra-high-throughput microbial community analysis on the Illumina HiSeq and MiSeq platforms. *The ISME journal* **6**: 1621–1624.

Christner, B.C. (2002) Incorporation of DNA and Protein Precursors into Macromolecules by Bacteria at -15oC. *Applied and Environmental Microbiology* **68**: 6435–6438.

Christner, B.C., Mikucki, J.A., Foreman, C.M., Denson, J., and Priscu, J.C. (2005) Glacial ice cores: A model system for developing extraterrestrial decontamination protocols. *Icarus* **174**: 572–584.

Dąbski, M. (2019) Should Glaciers Be Considered Permafrost? *Geosciences* **9**: 517.

Dieser, M., Broemsen, E.L.J.E., Cameron, K.A., King, G.M., Achberger, A., Choquette, K., et al. (2014) Molecular and biogeochemical evidence for methane cycling beneath the western margin of the Greenland Ice Sheet. *The ISME Journal* **8**: 2305–2316.

Dobinski, W. (2006) Ice and environment: A terminological discussion. *Earth-Science Reviews* **79**: 229–240.

Doyle, S., Dieser, M., Broemsen, E., and Christner, B. (2012) General characteristics of cold-adapted microorganisms. In *Polar Microbiology: Life in a Deep Freeze*. American Society of Microbiology, pp. 103–125.

Doyle, S., Montross, S., Skidmore, M., and Christner, B. (2013) Characterizing Microbial Diversity and the Potential for Metabolic Function at −15 °C in the Basal Ice of Taylor Glacier, Antarctica. *Biology* **2**: 1034–1053.

Filippidou, S., Wunderlin, T., Junier, T., Jeanneret, N., Dorador, C., Molina, V., et al. (2016) A Combination of Extreme Environmental Conditions Favor the Prevalence of Endospore-Forming Firmicutes. *Front Microbiol* **7**:.

Goordial, J., Davila, A., Lacelle, D., Pollard, W., Marinova, M.M., Greer, C.W., et al. (2016) Nearing the cold-arid limits of microbial life in permafrost of an upper dry valley, Antarctica. *The ISME Journal* **10**: 1613–1624.

Gow, A.J., Ueda, H.T., and Garfield, D.E. (1968) Antarctic Ice Sheet: Preliminary Results of First Core Hole to Bedrock. *Science* **161**: 1011–1013.

Hood, E., Fellman, J., Spencer, R.G.M., Hernes, P.J., Edwards, R., D'Amore, D., and Scott, D. (2009) Glaciers as a source of ancient and labile organic matter to the marine environment. *Nature* **462**: 1044–1047.

Hopwood, M.J., Carroll, D., Dunse, T., Hodson, A., Holding, J.M., Iriarte, J.L., et al. (2019) Review Article: How does glacier discharge affect marine biogeochemistry and primary production in the Arctic? *The Cryosphere Discussions* 1–51.

Hubbard, B., Cook, S., and Coulson, H. (2009) Basal ice facies: a review and unifying approach. *Quaternary Science Reviews* **28**: 1956–1969.

Itcus, C., Pascu, M.D., Lavin, P., Perşoiu, A., Iancu, L., and Purcarea, C. (2018) Bacterial and archaeal community structures in perennial cave ice. *Sci Rep* **8**:.

Janssen, S., McDonald, D., Gonzalez, A., Navas-Molina, J.A., Jiang, L., Xu, Z.Z., et al. (2018) Phylogenetic Placement of Exact Amplicon Sequences Improves Associations with Clinical Information. *mSystems* **3**: e00021-18.

Jung, J., Yoo, K.-C., Rosenheim, B.E., Conway, T.M., Lee, J.I., Yoon, H.I., et al. (2019) Microbial Fe(III) reduction as a potential iron source from Holocene sediments beneath Larsen Ice Shelf. *Nat Commun* **10**: 1–10.

Knight, P.G. (1997) The basal ice layer of glaciers and ice sheets. *Quaternary Science Reviews* **16**: 975–993.

Kochkina, G., Ivanushkina, N., Karasev, S., Gavrish, E.Y., Gurina, L., Evtushenko, L., et al. (2001) Survival of micromycetes and actinobacteria under conditions of long-term natural cryopreservation. *Microbiology* **70**: 356–364.

Korza, G., Setlow, B., Rao, L., Li, Q., and Setlow, P. (2016) Changes in Bacillus Spore Small Molecules, rRNA, Germination, and Outgrowth after Extended Sublethal Exposure to Various Temperatures: Evidence that Protein Synthesis Is Not Essential for Spore Germination. *J Bacteriol* **198**: 3254–3264.

Lacelle, D., Radtke, K., Clark, I.D., Fisher, D., Lauriol, B., Utting, N., and Whyte, L.G. (2011) Geomicrobiology and occluded O2–CO2–Ar gas analyses provide evidence of microbial respiration in ancient terrestrial ground ice. *Earth and Planetary Science Letters* **306**: 46–54.

Lamarche-Gagnon, G., Wadham, J.L., Sherwood Lollar, B., Arndt, S., Fietzek, P., Beaton, A.D., et al. (2019) Greenland melt drives continuous export of methane from the ice-sheet bed. *Nature* **565**: 73–77.

Lawson, D. (1979) Sedimentological Analysis of the Western Terminus Region of the Matanuska Glacier, Alaska. 132.

Lawson, D.E. and Kulla, J.B. (1978) An Oxygen Isotope Investigation of the Origin of the Basal Zone of the Matanuska Glacier, Alaska. *The Journal of Geology* **86**: 673–685.

Lawson, D.E., Strasser, J.C., Evenson, E.B., Alley, R.B., Larson, G.J., and Arcone, S.A. (1998) Glaciohydraulic supercooling: a freeze-on mechanism to create stratified, debris-rich basal ice: I. Field evidence. *Journal of Glaciology* **44**: 547–562.

Lee, J.E., Edwards, J.S., Schmitt, J., Fischer, H., Bock, M., and Brook, E.J. (2020) Excess methane in Greenland ice cores associated with high dust concentrations. *Geochimica et Cosmochimica Acta* **270**: 409–430.

McDonald, D., Price, M.N., Goodrich, J., Nawrocki, E.P., DeSantis, T.Z., Probst, A., et al. (2012) An improved Greengenes taxonomy with explicit ranks for ecological and evolutionary analyses of bacteria and archaea. *The ISME journal* **6**: 610.

Michaud, A.B., Dore, J.E., Achberger, A.M., Christner, B.C., Mitchell, A.C., Skidmore, M.L., et al. (2017) Microbial oxidation as a methane sink beneath the West Antarctic Ice Sheet. *Nature Geoscience* **10**: 582–586.

Mirarab, S., Nguyen, N., and Warnow, T. (2012) SEPP: SATé-enabled phylogenetic placement. In *Biocomputing 2012*. World Scientific, pp. 247–258.

Miteva, V., Rinehold, K., Sowers, T., Sebastian, A., and Brenchley, J. (2015) Abundance, viability and diversity of the indigenous microbial populations at different depths of the NEEM Greenland ice core. *Polar Research* **34**: 25057.

Miteva, V., Sowers, T., Schüpbach, S., Fischer, H., and Brenchley, J. (2016) Geochemical and Microbiological Studies of Nitrous Oxide Variations within the New NEEM Greenland Ice Core during the Last Glacial Period. *Geomicrobiology Journal* **33**: 647–660.

Miteva, V.I., Sheridan, P.P., and Brenchley, J.E. (2004) Phylogenetic and Physiological Diversity of Microorganisms Isolated from a Deep Greenland Glacier Ice Core. *Applied and Environmental Microbiology* **70**: 202–213.

Monteux, S., Weedon, J.T., Blume-Werry, G., Gavazov, K., Jassey, V.E.J., Johansson, M., et al. (2018) Long-term in situ permafrost thaw effects on bacterial communities and potential aerobic respiration. *The ISME Journal* **12**: 2129–2141.

Montross, S., Skidmore, M., Christner, B., Samyn, D., Tison, J.-L., Lorrain, R., et al. (2014) Debris-Rich Basal Ice as a Microbial Habitat, Taylor Glacier, Antarctica. *Geomicrobiology Journal* **31**: 76–81.

Montross, S.N. (2012) Biogeochemistry of basal ice from Taylor Glacier, Antarctica, Montana State University.

Montross, S.N., Skidmore, M., Tranter, M., Kivimaki, A.-L., and Parkes, R.J. (2013) A microbial driver of chemical weathering in glaciated systems. *Geology* **41**: 215–218.

Panikov, N.S., Flanagan, P.W., Oechel, W.C., Mastepanov, M.A., and Christensen, T.R. (2006) Microbial activity in soils frozen to below −39°C. *Soil Biology and Biochemistry* **38**: 785–794.

Perreault, N.N., Greer, C.W., Andersen, D.T., Tille, S., Lacrampe-Couloume, G., Lollar, B.S., and Whyte, L.G. (2008) Heterotrophic and Autotrophic Microbial Populations in Cold Perennial Springs of the High Arctic. *Appl Environ Microbiol* **74**: 6898–6907.

Priscu, J.C., Tulaczyk, S., Studinger, M., Kennicutt, M., Christner, B.C., and Foreman, C.M. (2008) Antarctic subglacial water: origin, evolution and ecology. *Polar lakes and rivers: limnology of Arctic and Antarctic aquatic ecosystems Oxford University Press, Oxford* 119–135.

Quast, C., Pruesse, E., Yilmaz, P., Gerken, J., Schweer, T., Yarza, P., et al. (2013) The SILVA ribosomal RNA gene database project: improved data processing and web-based tools. *Nucleic Acids Research* **41**: D590–D596.

Rhodes, R.H., Faïn, X., Stowasser, C., Blunier, T., Chappellaz, J., McConnell, J.R., et al. (2013) Continuous methane measurements from a late Holocene Greenland ice core: Atmospheric and in-situ signals. *Earth and Planetary Science Letters* **368**: 9–19.

Rignot, E. and Jacobs, S.S. (2002) Rapid Bottom Melting Widespread near Antarctic Ice Sheet Grounding Lines. *Science* **296**: 2020–2023.

Salter, S.J., Cox, M.J., Turek, E.M., Calus, S.T., Cookson, W.O., Moffatt, M.F., et al. (2014) Reagent and laboratory contamination can critically impact sequence-based microbiome analyses. *BMC biology* **12**: 87.

Segev, E., Smith, Y., and Ben-Yehuda, S. (2012) RNA Dynamics in Aging Bacterial Spores. *Cell* **148**: 139–149.

Sharp, M., Parkes, J., Cragg, B., Fairchild, I.J., Lamb, H., and Tranter, M. (1999) Widespread bacterial populations at glacier beds and their relationship to rock weathering and carbon cycling. *Geology* **27**: 107.

Sheridan, P.P., Miteva, V.I., and Brenchley, J.E. (2003) Phylogenetic Analysis of Anaerobic Psychrophilic Enrichment Cultures Obtained from a Greenland Glacier Ice Core. *Applied and Environmental Microbiology* **69**: 2153–2160.

Skidmore, M.L., Foght, J.M., and Sharp, M.J. (2000) Microbial Life beneath a High Arctic Glacier. *Appl Environ Microbiol* **66**: 3214–3220.

Spirina, E., Durdenko, E., Demidov, N., Abramov, A., Romanovsky, V., and Rivkina, E. (2017) Halophilic-psychrotrophic bacteria of an Alaskan cryopeg—a model for astrobiology. *Paleontological Journal* **51**: 1440–1452.

Steven, B., Briggs, G., McKay, C.P., Pollard, W.H., Greer, C.W., and Whyte, L.G. (2007) Characterization of the microbial diversity in a permafrost sample from the Canadian high Arctic using culture-dependent and culture-independent methods: Microbial diversity in Canadian high Arctic permafrost. *FEMS Microbiology Ecology* **59**: 513–523.

Steven, B., Pollard, W.H., Greer, C.W., and Whyte, L.G. (2008) Microbial diversity and activity through a permafrost/ground ice core profile from the Canadian high Arctic. *Environmental Microbiology* **10**: 3388–3403.

Stibal, M., Wadham, J.L., Lis, G.P., Telling, J., Pancost, R.D., Dubnick, A., et al. (2012) Methanogenic potential of Arctic and Antarctic subglacial environments with contrasting organic carbon sources. *Global Change Biology* **18**: 3332–3345.

Strasser, J.C., Lawson, D.E., Larson, G.J., Evenson, E.B., and Alley, R.B. (1996) Preliminary results of tritium analyses in basal ice, Matanuska Glacier, Alaska, U.S.A.: evidence for subglacial ice accretion. *Annals of Glaciology* **22**: 126–133.

Tranter, M., Sharp, M.J., Lamb, H.R., Brown, G.H., Hubbard, B.P., and Willis, I.C. (2002) Geochemical weathering at the bed of Haut Glacier d'Arolla, Switzerland?a new model. *Hydrological Processes* **16**: 959–993.

Tranter, M., Skidmore, M., and Wadham, J. (2005) Hydrological controls on microbial communities in subglacial environments. *Hydrological Processes* **19**: 995–998.

Tung, H. c., Price, P. b., Bramall, N. e., and Vrdoljak, G. (2006) Microorganisms Metabolizing on Clay Grains in 3-Km-Deep Greenland Basal Ice. *Astrobiology* **6**: 69–86.

Vick-Majors, T.J., Michaud, A.B., Skidmore, M.L., Turetta, C., Barbante, C., Christner, B.C., et al. (2020) Biogeochemical Connectivity Between Freshwater Ecosystems beneath the West Antarctic Ice Sheet and the Sub-Ice Marine Environment. *Global Biogeochemical Cycles* **34**: e2019GB006446.

Wadham, J.L., Arndt, S., Tulaczyk, S., Stibal, M., Tranter, M., Telling, J., et al. (2012) Potential methane reservoirs beneath Antarctica. *Nature* **488**: 633–637.

Wadham, J.L., Bottrell, S., Tranter, M., and Raiswell, R. (2004) Stable isotope evidence for microbial sulphate reduction at the bed of a polythermal high Arctic glacier. *Earth and Planetary Science Letters* **219**: 341–355.

Wadham, J.L., Tranter, M., Skidmore, M., Hodson, A.J., Priscu, J., Lyons, W.B., et al. (2010) Biogeochemical weathering under ice: Size matters: GLACIAL BIOGEOCHEMICAL WEATHERING. *Global Biogeochemical Cycles* **24**: n/a-n/a.

822 Wang, Q., Garrity, G.M., Tiedje, J.M., and Cole, J.R. (2007) Naïve Bayesian Classifier for Rapid
823 Assignment of rRNA Sequences into the New Bacterial Taxonomy. *Appl Environ*
824 *Microbiol* **73**: 5261–5267.
825 Yde, J.C., Finster, K.W., Raiswell, R., Steffensen, J.P., Heinemeier, J., Olsen, J., et al. (2010)
826 Basal ice microbiology at the margin of the Greenland ice sheet. *Annals of Glaciology*
827 **51**: 71–79.
828 Yung, P.T., Shafaat, H.S., Connon, S.A., and Ponce, A. (2007) Quantification of viable
829 endospores from a Greenland ice core: Quantification of viable endospores from a
830 Greenland ice core. *FEMS Microbiology Ecology* **59**: 300–306.
831 Zdanowski, M.K., Bogdanowicz, A., Gawor, J., Gromadka, R., Wolicka, D., and Grzesiak, J.
832 (2017) Enrichment of Cryoconite Hole Anaerobes: Implications for the Subglacial
833 Microbiome. *Microb Ecol* **73**: 532–538.
834

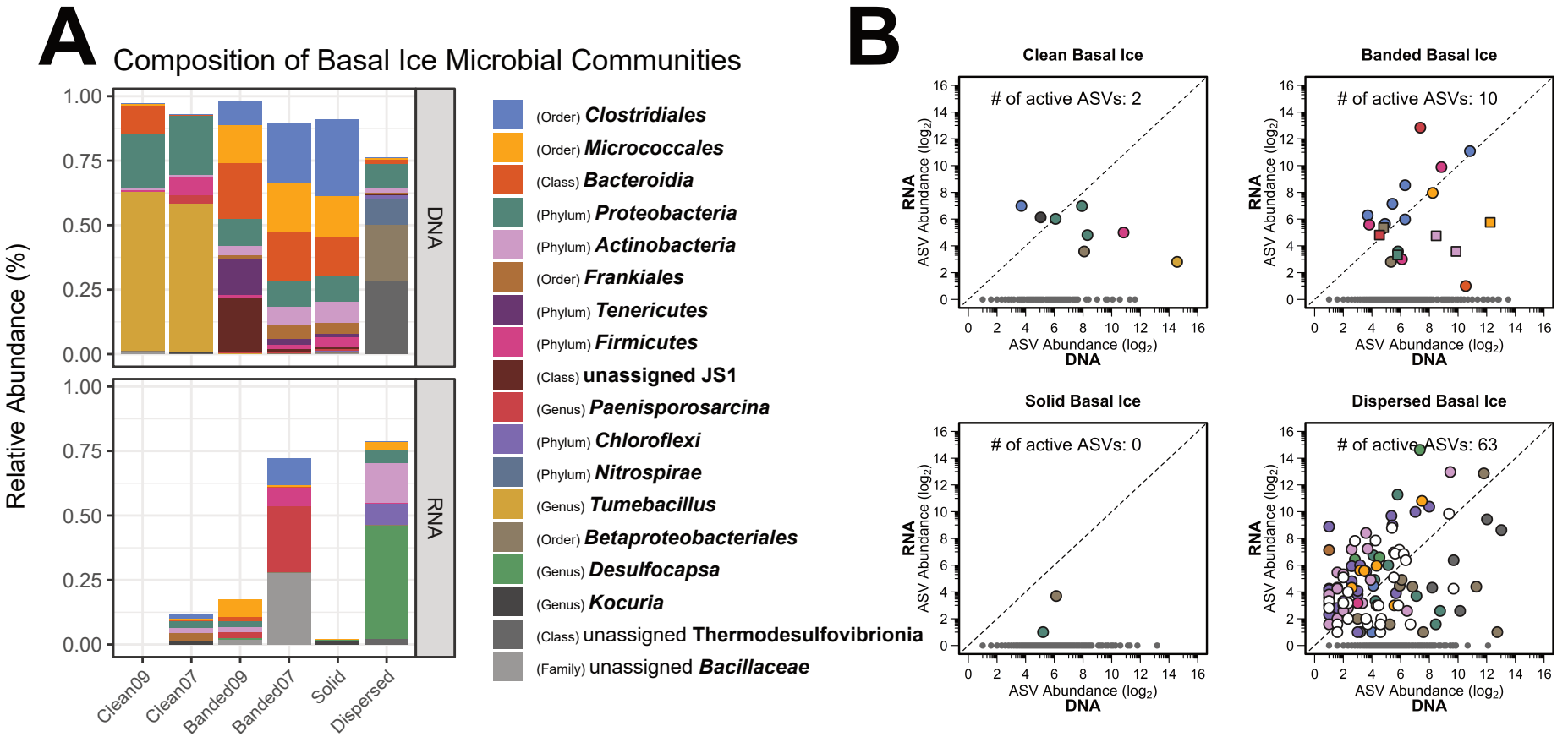

Figure 1. [A] Relative abundances of microbial lineages observed in basal ice using both DNA and RNA for detecting 16S rRNA sequences. The graph displays the highest resolution classification for the most abundant taxa and was constructed as follows: First, ASVs were clustered by genus and any having a relative abundance ≥20% in at least one of the samples were plotted. This procedure was subsequently repeated with the remaining unplotted ASVs at the rank of family, order, class, and finally phylum. Any remaining rare taxa left after this procedure were not plotted. The bottom plot was scaled to reduce inflated relative abundance biases introduced during curation. **[B]** Scatter plots of potentially active ASVs within four types of basal ice. Each point represents an ASV. Points falling on the dotted-line are equally abundant in both the DNA- and RNA-based 16S rRNA library. Gray points denote those ASVs observed only in the DNA-based libraries. In the banded basal ice plot, circles denote ASVs from the Banded07 sample while squares denote ASVs from the Banded09 sample. The # of active ASVs in each plot denotes the number of ASVs falling above the x=y line.

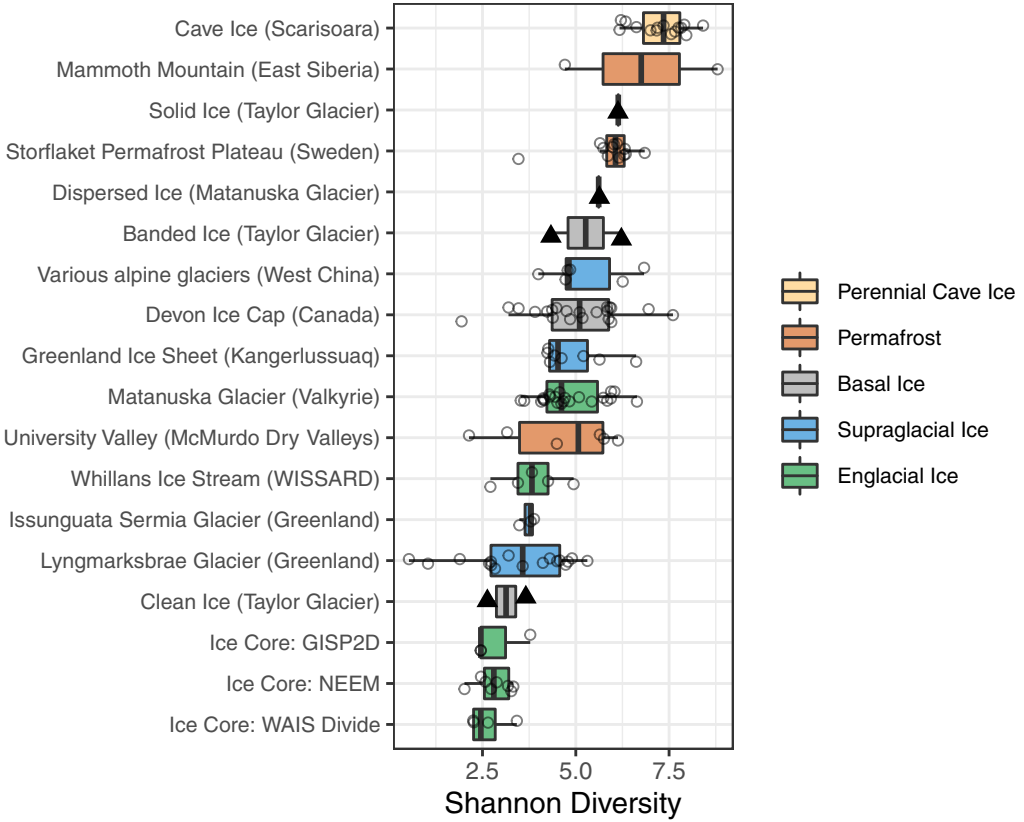

Figure 2. Microbial alpha diversity (Shannon) within various permanently frozen environments.

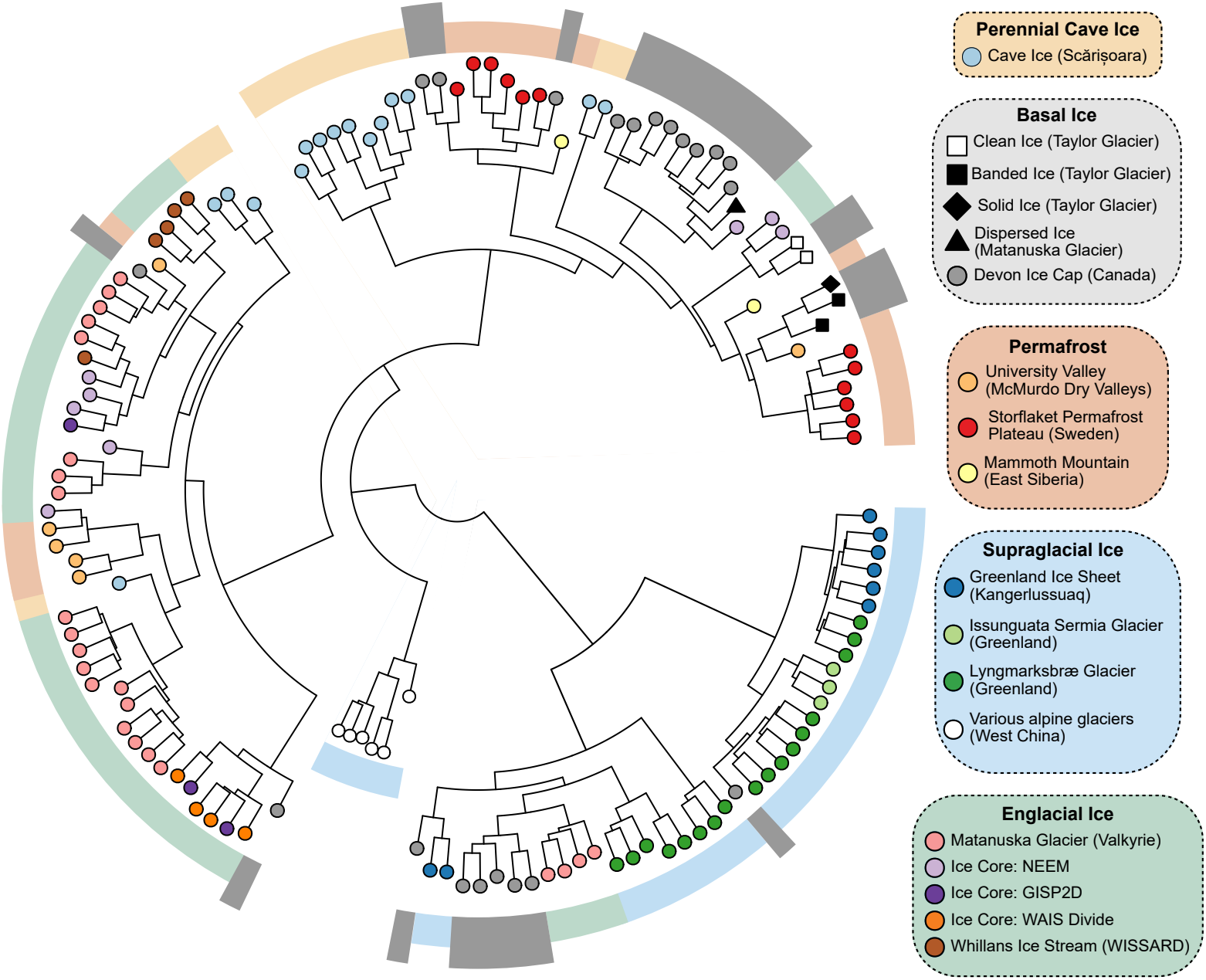

Figure 3. Hierarchical cluster analysis of wUF distances between samples using Ward's minimum variance method.

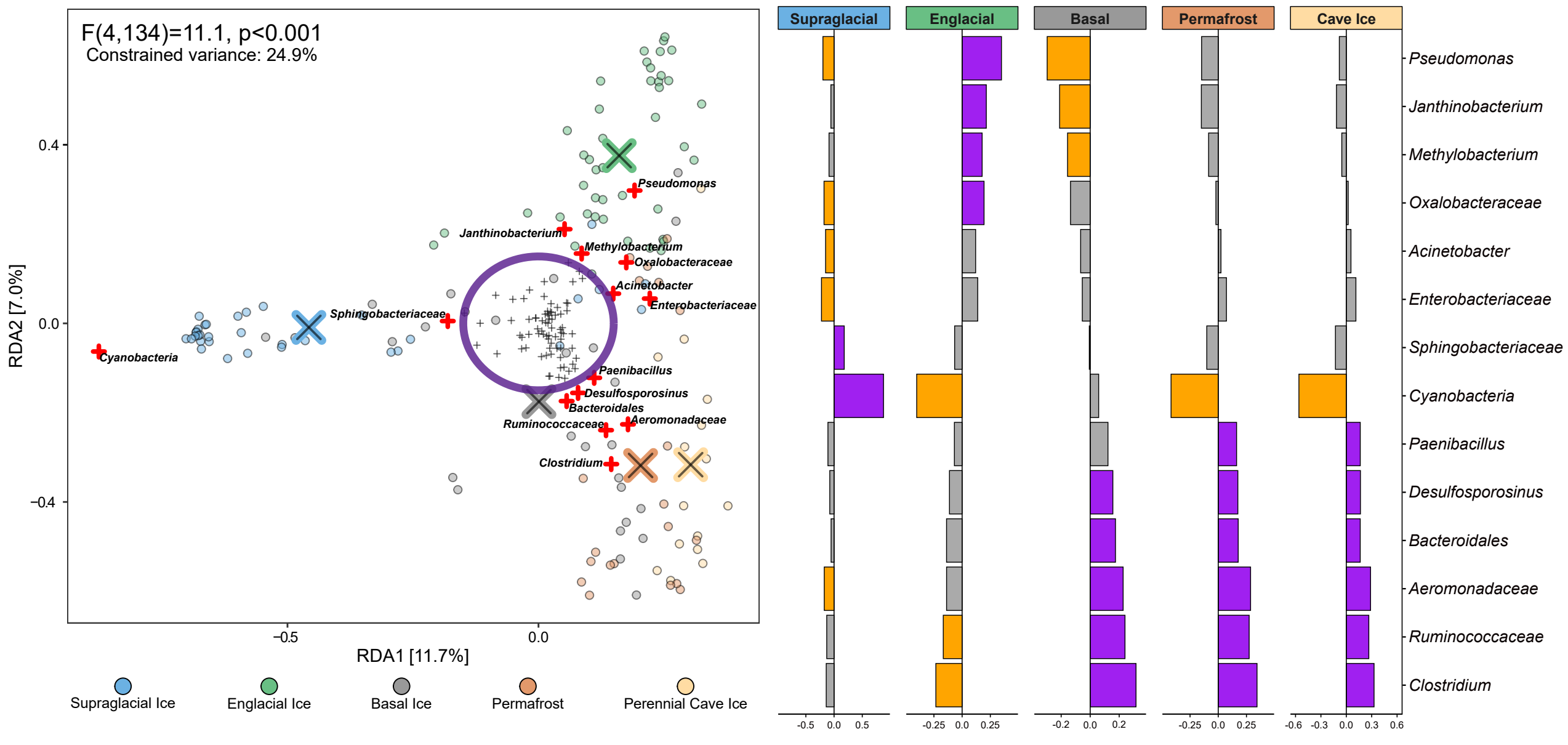

Figure 4. [Left] RDA triplot of the distribution of 89 microbial lineages across five different permanently frozen environments. Colored circles represent individual samples. Centroids of each sample type are indicated with an "×". Plus signs (+) represent microbial lineages. The purple circle denotes the equilibrium contribution of the overall model and delineates lineages which substantially constrained the overall ordination. Those lineages are highlighted in red. **[Right]** Magnitude of the scalar projections of these 14 lineages onto the centroids for each ice types approximates that lineage's association with that frozen environment. Scalar projections smaller than the equilibrium contribution were considered inconclusive and marked gray. Positive and negative associations are purple and orange, respectively.

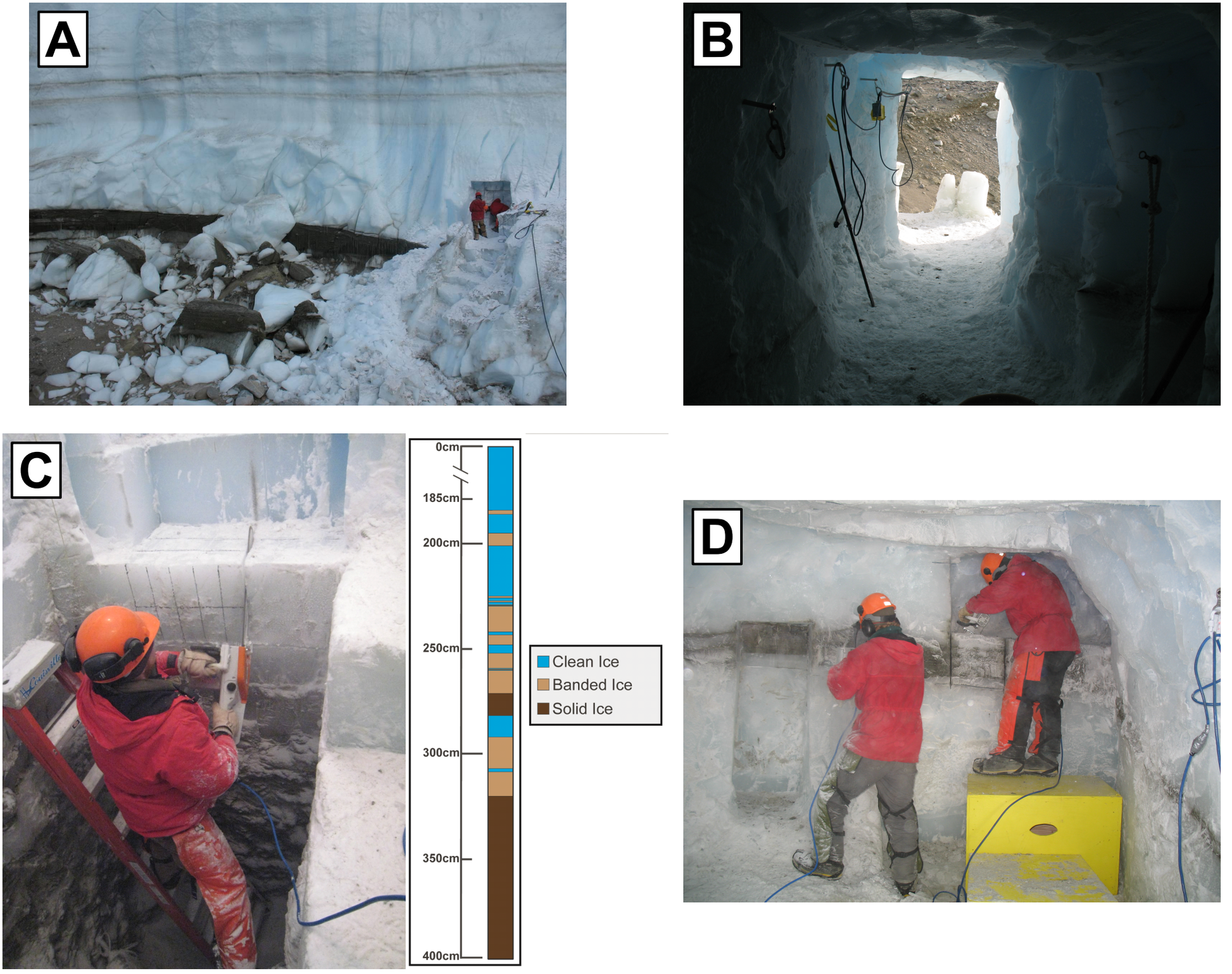

Figure S1. [A] A subglacial tunnel was excavated into the basal zone of Taylor Glacier's northern lateral margin. **[B]** View from inside one of the excavation tunnels. **[C]** During the 2007 expedition, a vertical shaft was excavated and stratigraphic sequence of multiple basal ice types was sampled. **[D]** During the 2009 expedition, a large chamber was excavated to sample a horizon of debris-rich banded basal ice.

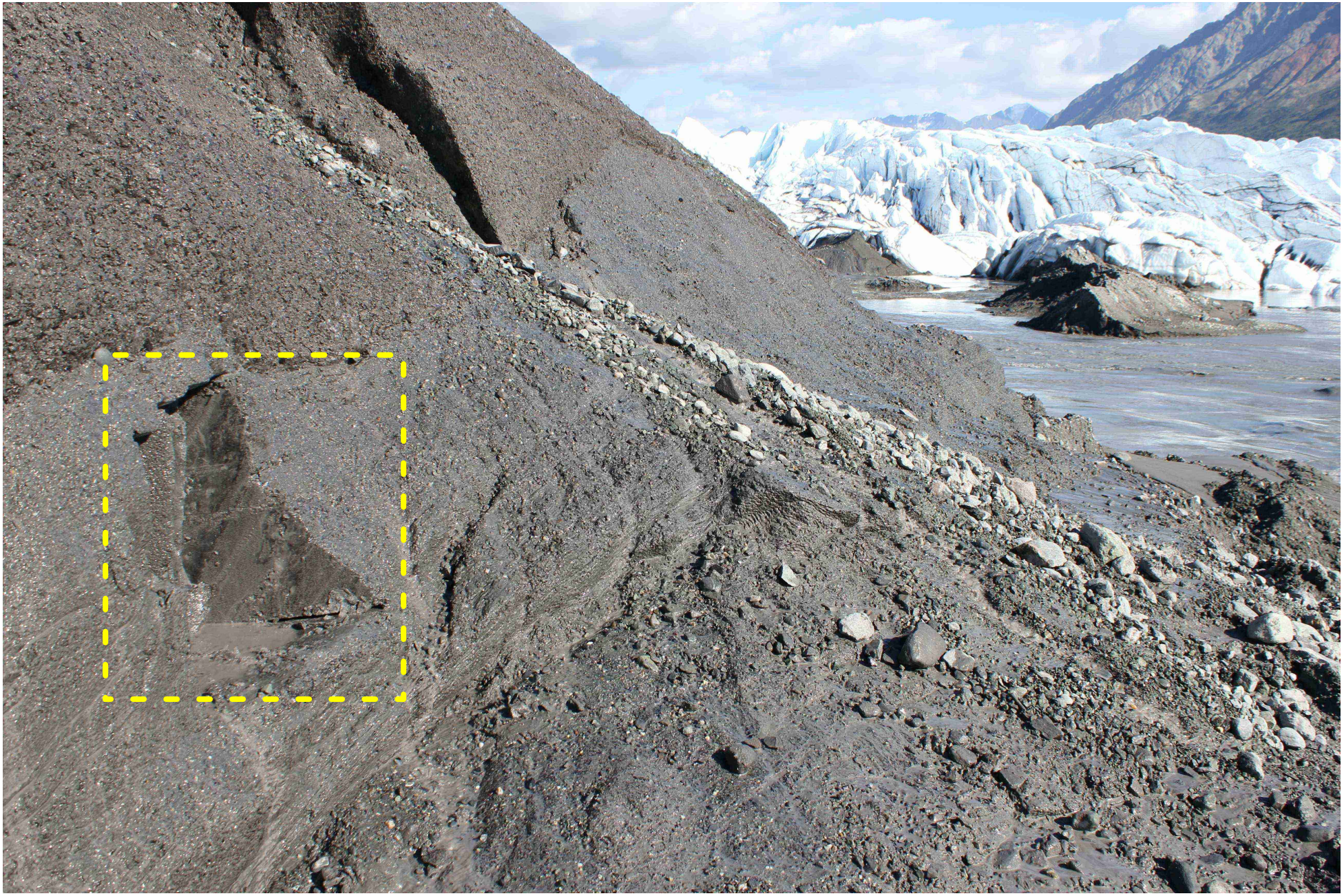

Figure S2. An exposed horizon debris-rich basal ice near the terminus of Matanuska Glacier, Alaska. The sampled area, collected using an electric chainsaw, is highlighted inside the yellow-box.

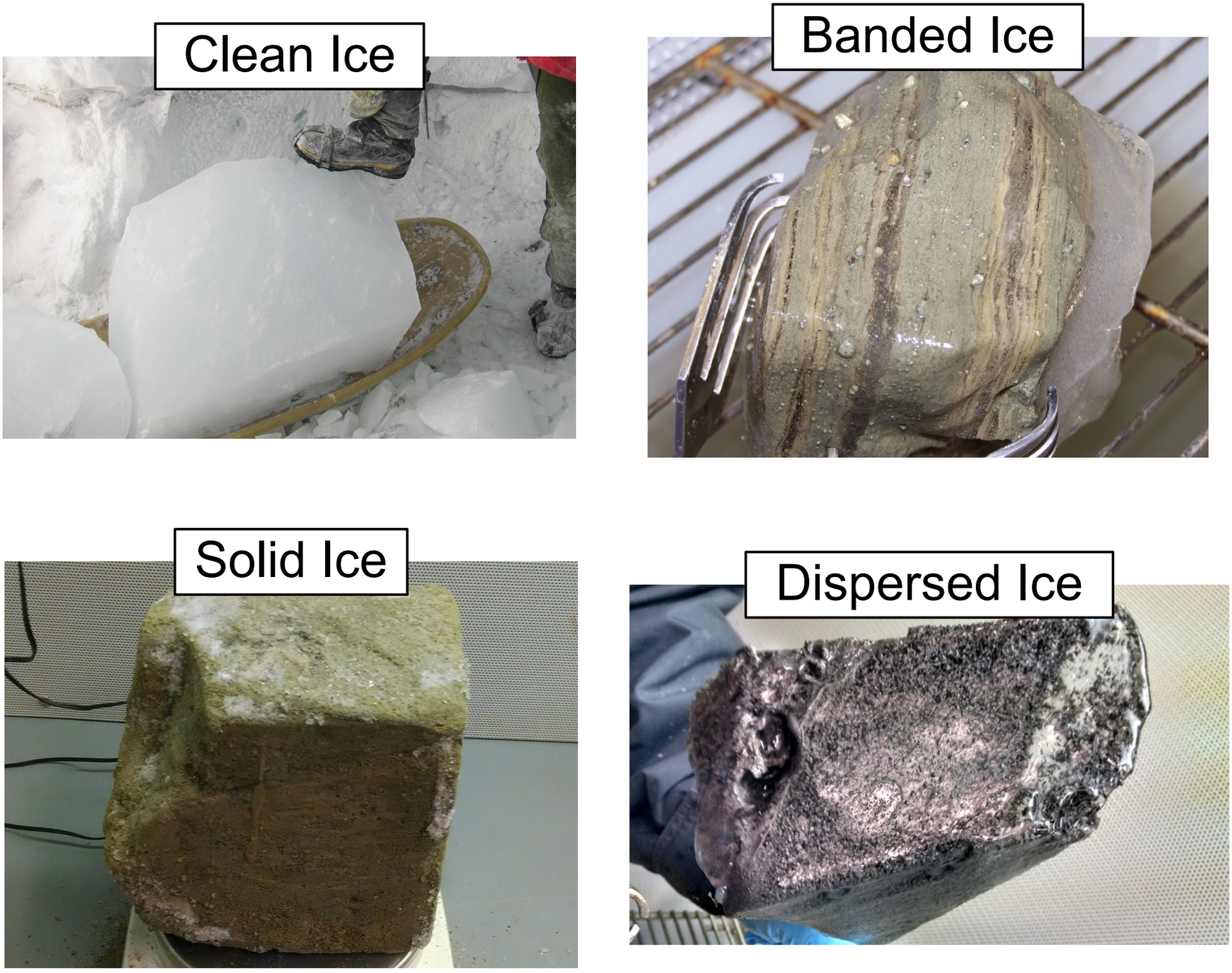

Figure S3. Examples of each type of basal ice analyzed in this study. Clean ice, banded ice, and solid ice were collected from Taylor Glacier, Antarctica. Dispersed ice was collected from Matanuska Glacier, Alaska.